# Tunable Control of the Hydrophilicity and Wettability of Conjugated Polymers by a Postpolymerization Modification Approach

*Shengyu Cong, Adam Creamer, Zhuping Fei, Sam A. J. Hillman, Charlotte Rapley, Jenny Nelson, and Martin Heeney\**

A facile method to prepare hydrophilic polymers by a postpolymerization nucleophillic aromatic substitution reaction of fluoride on an emissive conjugated polymer (CP) backbone is reported. Quantitative functionalization by a series of monofunctionalized ethylene glycol oligomers, from dimer to hexamer, as well as with high molecular weight polyethylene glycol is demonstrated. The length of the ethylene glycol sidechains is shown to have a direct impact on the surface wettability of the polymer, as well as its solubility in polar solvents. However, the energetics and band gap of the CPs remain essentially constant. This method therefore allows an easy way to modulate the wettability and solubility of CP materials for a diverse series of applications.

## 1. Introduction

Conjugated polymers (CPs) are a class of organic materials that have delocalized aromatic backbones and unique electronic and optical properties.[1–3] They have been widely investigated for application in a range of optoelectronic devices such as organic light-emitting diodes and organic field-effect transistors.[4,5] More recently the application of CPs in the bioelectronic field has attracted much interest.[6–8] For example, CPs have been used as electrically active tissue engineering scaffolds which can control protein conformation and cell adhesion.[9,10] They

have also found application as the active material in electrochemical transistors, where their mixed electronic and ionic conductivity is utilized.[11] This has been further leveraged in organic electronic ion pumps to control drug delivery.[12] Also, CPs have been used as biosensors such as glucose monitors for diabetics[13] and as implants for the restoration of physiological functions.[14] The potential advantages of CPs over more traditional conductors and semiconductors in bioelectronics can be found in their facile chemical functionalization[15] and potential low temperature processing.[16] In addition, CPs are soft, flexible, and mechanically tuneable, with a better match to the mechanical properties of biological tissue than traditional conductors and inorganic semiconductors.[17,18]

Most common CPs are hydrophobic and only soluble in organic solvents. In order to function in many of bioelectronic devices it is important that the CP can support ionic as well as electronic transport at room temperature. Most bioelectronic devices to date depend on well-established CPs such as doped polypyrrole (Ppy),[19] doped polyaniline,[20] and polythiophene derivatives such as poly(3,4-ethylenedioxythiophene) doped with poly(styrenesulfonate) (PEDOT:PSS).[21] However these materials have some drawbacks and processability challenges.[7,16] In order to overcome these challenges, more recent work has shown that the incorporation of ionic or ethylene glycol based sidechains onto the backbone of the CP can promote ionic conductivity,[22,23] although the performance has been shown to be very sensitive to relative percentage of hydrophobic/hydrophilic groups on the backbone.[24] The addition of ethylene glycol chains to CPs has also been shown to promote closer $\pi$-stacking of conjugated backbones,[25,26] enhance the dielectric constant,[27,28] and afford higher charge carrier mobility in transistor devices[29,30] compared to the analogous alkylated polymers.

In addition to ion conductivity, another important aspect for many bioelectronic devices is the interface between biological tissue and the CP at the cellular level.[31] The surface of the CP must allow effective cell adhesion and support for cells to establish intimate contact with living tissue.[32,33] Cell adhesion to organic materials is affected by their surface properties such as wettability, roughness, surface charge, and chemical functionality.[34–36] Among these properties, surface wettability has been most extensively investigated, with cells found to adhere more effectively onto surfaces with moderate wettability than hydrophobic surfaces.[37–40]

Dr S. Cong, Dr A. Creamer, C. Rapley, Prof. M. Heeney
Department of Chemistry and Centre for Processable Electronics
Imperial College London
White City Campus, London W12 0BZ, UK
E-mail: m.heeney@imperial.ac.uk
S. A. J. Hillman, Prof J. Nelson
Department of Physics and Centre for Processable Electronics
Imperial College London
South Kensington Campus, London SW7 2AZ, UK
Prof. Z. Fei
Institute of Molecular Plus
Tianjin Key Laboratory of Molecular Optoelectronic Science
Tianjin University
Tianjin 300072, P. R. China

**ADVANCED
SCIENCE NEWS**
www.advancedsciencenews.com

**Macromolecular
Bioscience**
www.mbs-journal.de

Factors such as cell types, surface functionalization, and roughness are also important.[36] Thus in order to fulfil diverse cell adhesion, easy control of surface wettability is required.

In addition to their role in bioelectronic devices, the highly emissive nature of many CPs has led to their investigation as fluorescent probes for various analytes and biomolecules.[41,42] Solubility of the CP in aqueous media is again essential for interfacing with the biomacromolecules.[43] However, current approaches to make suitably functionalized CPs are relatively laborious, with hydrophilic sidechains (often charged groups or ethylene glycol oligomers) usually introduced at an early stage of the monomer synthesis.[44] Investigating the optimal length and nature of the hydrophilic sidechains on the CP backbone therefore requires significant synthetic effort. Furthermore control of the percentage hydrophilic/hydrophobic groups is typically achieved by copolymerization approaches,[24,45] in which it can be difficult to achieve similar molecular weights and dispersities to allow fair comparison between copolymers.

Recently we reported an approach to directly functionalize the backbone of a CP by a nucleophilic aromatic substitution ($S_NAr$) reaction of an electron-deficient fluorinated co-monomer.[46] This allowed the quantitative incorporation of a range of functional groups onto the polymer backbone. Here we expand upon that work to report an effective and facile approach to control the hydrophilicity and wettability of CPs by a postpolymerization modification protocol. We demonstrate that this method can readily graft different lengths of ethylene glycol sidechains (from dimers to hexamers) to the conjugated backbone, allowing fine control of the surface wettability of thin films. A polymer containing a branched alkyl group (2-ethylhexyloxyl) was also prepared as a control, to examine the effect of the ether functionalization without the presence of polar ethylene glycol groups. Furthermore monofunctional polymers of ethyene glycol of high molecular weight ($M_n = 10\,000$ g mol$^{-1}$) were also grafted to the conjugated backbone to afford fully water-soluble conjugated graft-copolymers. We believe this method opens up a way to control wettability and hydrophilicity of a range of CPs.

## 2. Results and Discussion

### 2.1. Synthesis

Our starting point for the investigation was a derivative of the well-known emissive polymer F8BT (poly(dioctylfluorene-co-benzothiadiazole)),[47] in which the benzothiadiazole was replaced with a fluorinated benzothiadiazole (FBT).[48] We had previously shown that the resulting polymer F8FBT was amenable to direct displacement of the fluoride group under nucleophillic aromatic substitution conditions.[46] The starting materials, 2,7-dibromo-9,9-dioctylfluorene (**2**) and 9,9-dioctyl-9H-fluorene-2,7-diboronic acid bis (pinacol) ester (**3**) were synthesized according to the literature.[49] Under typical Suzuki reaction conditions, equimolar quantities of (**3**) were reacted with 4,7-dibromo-5-fluorobenzo-2,1,3-thiadiazole to give F8FBT (**Scheme 1**). After reaction, the polymer was purified by Soxhlet washing with methanol, acetone, and hexane to remove lower molecular weight oligomers and catalyst residues. The resultant F8FBT was soluble in typical organic solvents such as toluene, tetrahydrofuran

(THF), chloroform, and chlorobenzene at room temperature. Molecular weight analysis by gel permeation chromatography (GPC) indicated $M_n = 38\,500$ g mol$^{-1}$ and $M_w = 65\,100$ g mol$^{-1}$ ($Đ = M_w/M_n$: 1.69) versus polystyrene standards.

Following successful synthesis of F8FBT, the fluoride displacement reactions were optimized based on our previous protocol. Typically aprotic solvents perform best for $S_NAr$ reactions, but F8FBT was not soluble in dimethyl sulfoxide (DMSO) alone. Therefore, a mixture of chlorobenzene and DMSO was utilized in the presence of KOH and excess ethylene glycol at 120 °C. The nucleophilic aromatic substitution reactions were monitored by $^{19}$F-NMR spectroscopy of quenched aliquots. It is worth noting that no reaction with KOH in the absence of ethylene glycol was observed. The reactions were complete when $^{19}$F-NMR did not show any fluorine signal, typically after 48 h, in good isolated yields.

After reaction, the products were precipitated into methanol, then purified by Soxhlet washing with acetone (24 h) under nitrogen to give the substituted polymers. However, F8BT-PEG was soluble in methanol due to the grafted hydrophilic polyethylene glycol (PEG$_{10K}$). Hence for F8BT-PEG, the reaction solvent was removed under reduced pressure and the residue was dissolved in deionized water. The excess PEG was removed by dialysis for 2 d and pure F8BT-PEG was obtained. All substituted polymers are characterized by $^1$H and $^{19}$F-NMR.

Diffusion ordered NMR spectroscopy (DOSY) was used to confirm the coupling of the polymeric PEG ($M_n = 10\,000$ g mol$^{-1}$) with the F8FBT backbone and to confirm the purity of the graft copolymer. In DOSY each component in a mixture can be pseudo-separated, based on its own diffusion coefficient.[50] A physical mixture of F8FBT and PEG$_{10K}$ was investigated initially by DOSY (Figure S1, Supporting Information). In addition to the solvent, clear signals from PEG and F8FBT were observed, with obviously different diffusion coefficients (values were not calibrated). The corresponding DOSY spectra of the graft copolymer F8BT-PEG, although nonquantitative, afforded a single diffusion constant, indicating the successful synthesis of F8BT-PEG (Figure S2, Supporting Information). Given the synthetic challenge of successfully coupling polymers to one another, this truly demonstrates the utility of the methodology.

The molecular weights of the polymers were all determined by GPC in chlorobenzene and are summarized in **Table 1**. As the substituted polymers are all from the same batch of F8FBT, we would expect an increasing $M_w/M_n$ as the mass of the sidechain increases, with a similar dispersity for all polymers, although some small variance may occur due to the work-up and purification. The calculated degree of polymerization for each polymer is also included in Table 1. Indeed the observed $M_n$ and $M_w$ gradually increases as the length of the hydrophilic chain is increased from diethylene glycol monomethyl ether (m = 2) to tetraethyleneglycol monomethyl ether (m = 4), before decreasing for pentaethyleneglycol monomethyl ether (m = 5) and hexaethylene glycol (m = 6). The hydrophobic ethylhexyloxy chain exhibited a similar profile to the starting polymer. We believe these changes are related to differences in the hydrodynamic radius in solution as the side chain length and polarity changes. We further note that we could observe no signal for graft polymer F8BT-PEG by GPC under these conditions, likely due to the adsorption of F8BT-PEG onto the surface of GPC stationary phase.
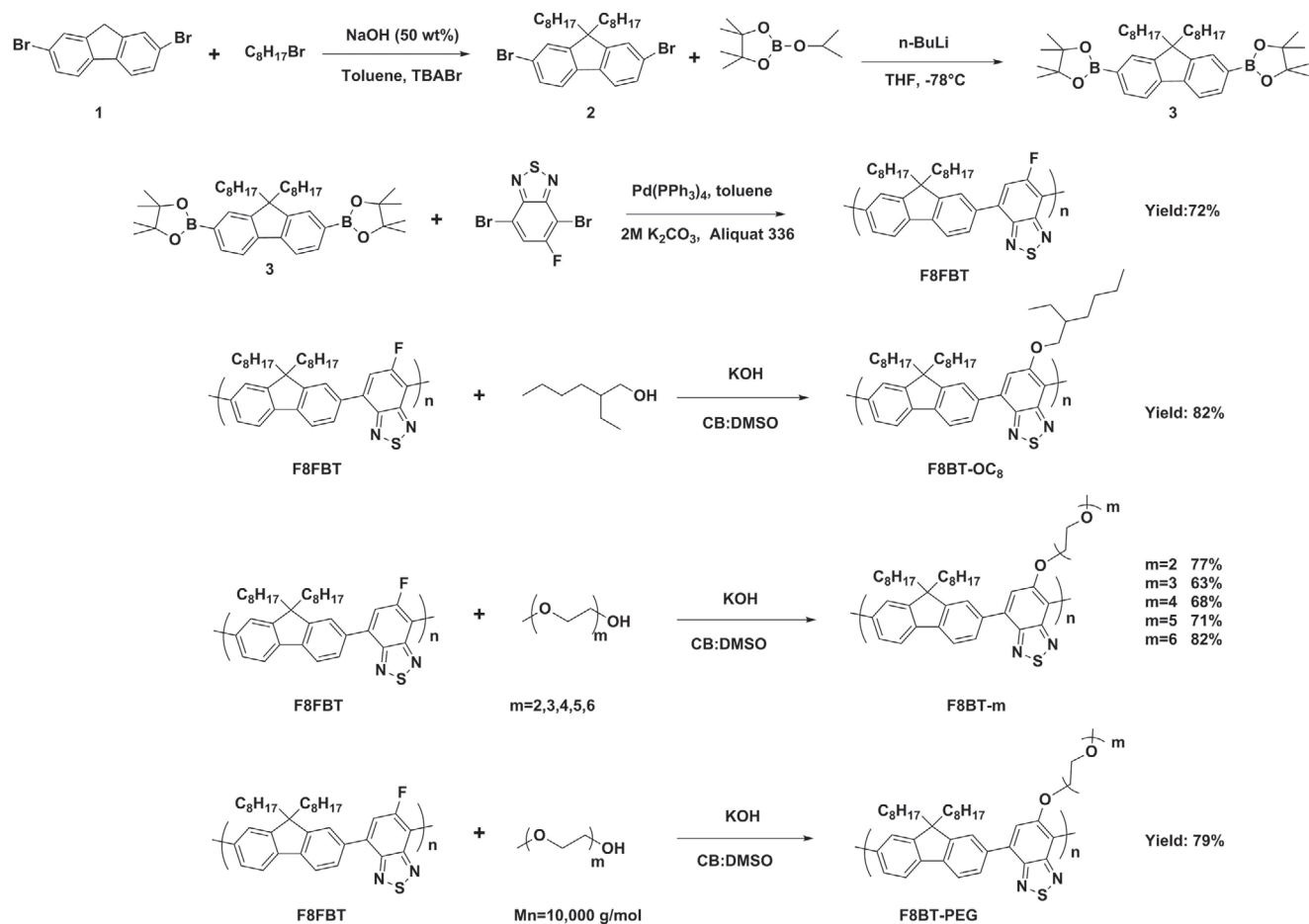
**Scheme 1.** Synthesis of monomers and substituted polymers.

## 2.2. Optoelectronic Properties

The UV-Vis absorption spectra of F8FBT, F8BT-OC$_8$, F8BT-m (m = 2, 3, 4, 5, 6), and F8BT-PEG at room temperature in chloroform solution and as thin films are shown in **Figure 1** and the data summarized in **Table 2**. The spectra are similar to

**Table 1.** Molecular weights of polymers (polystyrene as standards, chlorobenzene as solvent).

| Polymer | M$_n$[KDa] | M$_w$[KDa] | DP$_n$ [a] | DP$_w$ [b] | Đ [c] |
|---|---|---|---|---|---|
| F8FBT | 38.5 | 65.1 | 71 | 120 | 1.69 |
| F8BT-OC$_8$ | 37.5 | 74.2 | 57 | 113 | 1.98 |
| F8BT-2 | 45.4 | 78.3 | 70 | 121 | 1.72 |
| F8BT-3 | 54.1 | 59.3 | 78 | 129 | 1.65 |
| F8BT-4 | 55.2 | 88.1 | 75 | 120 | 1.60 |
| F8BT-5 | 50.8 | 83.9 | 66 | 110 | 1.65 |
| F8BT-6 | 49.9 | 85.4 | 62 | 107 | 1.71 |
| F8BT-PEG | – | – | – | – | – |

[a] Degree of polymerization calculated from M$_n$; [b] Degree of polymerization calculated from M$_w$; [c] Đ calculated from M$_w$/M$_n$.

the parent F8BT polymer,[47] with all polymers exhibiting two absorption bands in solution and thin films: a high energy band corresponding to the $\pi$–$\pi^*$ transition and a low energy band corresponding to intramolecular charge transfer (ICT) to the electron-deficient benzothiadiazole monomer.[51] The parent F8FBT exhibits peaks at 319 and 440 nm in chloroform, similar to the reported spectrum.[48] Substitution of the electron-withdrawing fluoride with the electron-donating ether group results in a slight red-shift of both bands in all examples (Table 2), as well a reduction in the relative intensity of the ICT band with respect to the high energy band, likely as a result of the weakening of the electron-accepting ability of the benzothiadiazole. All of the ether functionalized polymers exhibited similar spectra, highlighting that the length of chain has little influence on the polymer bandgap. A similar trend is apparent in the solid state, with all ether functionalized polymers exhibiting remarkably similar spectra, even for the polymer with long PEG chains. A slight weakening of the relative intensity of the ICT peak for F8BT-PEG polymer is maybe due to the weaker interchain interactions caused by the very long side chain.[52] Optical band gaps, as measured by the onset of absorption, are 2.44–2.46 eV in all cases.

The photoluminescence spectra of the polymers in chloroform solution and as thin films are shown in **Figure 2**. The
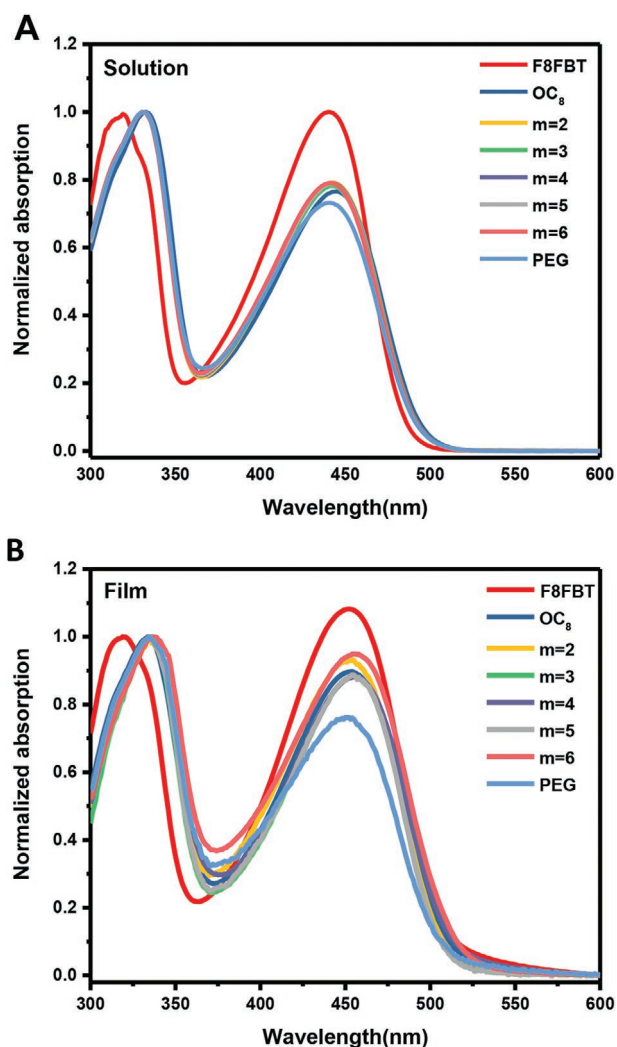
**Figure 1.** UV-Vis absorption spectra of polymers in chloroform solution a) and thin film b).

emission maxima ($\lambda_{em, max}$) of the polymer solutions and thin films are summarized in Table 2. F8FBT apart, all polymers show broad emission profiles with maxima in the green region of the spectrum ($\lambda_{em, max}$ of 546 nm), corresponding to

a Stokes shift of 104 nm and a red-shift of 14 nm compared to the parent F8FBT. All the ether-containing polymers have nearly identical emission profiles in chloroform solution. Upon moving to thin films, the ether-containing polymers again have very similar $\lambda_{em, max}$ (550–556 nm), which are slightly red-shifted compared to solution. The emission profiles of F8BT-3, -4, and -5 are slightly broader compared to other polymers.

The electronic properties of the substituted polymers were investigated using cyclic voltammetry (CV). Samples were prepared by drop-casting solution onto the surface of a Pt rod. Samples were measured in anhydrous, degassed solutions of acetonitrile with tetrabutylammonium hexafluorophosphate (0.1 M) electrolyte using an Ag/Ag$^+$ as reference electrode. The CV of all polymers are shown in Figure S3 (Supporting Information) and summarized in Table 2. The highest occupied molecular orbital (HOMO) level of each polymer was estimated from the onset of oxidation, assuming that the ferrocene/ferrocenium (FOC) reference redox system is 4.8 eV below the vacuum level.[53] The HOMO level of F8FBT was −6.09 eV, which is very similar to the reported value (−6.01 eV).[48] Substitution of the electron-deficient fluorine with the electron-donating ether group results an increase in the HOMO level of all functionalized polymers, to values between −5.77 and −5.67 eV. These values approximately identical, within the error of the measurement (± 0.1 eV),[54] and similar to the optical results show that changing the length of the sidechain does not have a significant impact on the electronic properties. We note that the thin-film CV of F8BT-PEG could not be measured, as it was soluble in acetonitrile.

### 2.3. Thermal Properties

Differential scanning calorimetry (DSC) has been widely applied to explore the crystallinity and thermal behavior of polymers. The thermal behavior of F8FBT, F8BT-OC$_8$, F8BT-m (m = 2, 3, 4, 5, 6), and F8BT-PEG was measured using DSC on powder samples under nitrogen (Figure S4, Supporting Information). For the parent F8FBT, we observe two overlapping endotherms on initial heating, with an onset at 226 °C and peaks at 243 °C and 262 °C. Upon cooling, an exothermic
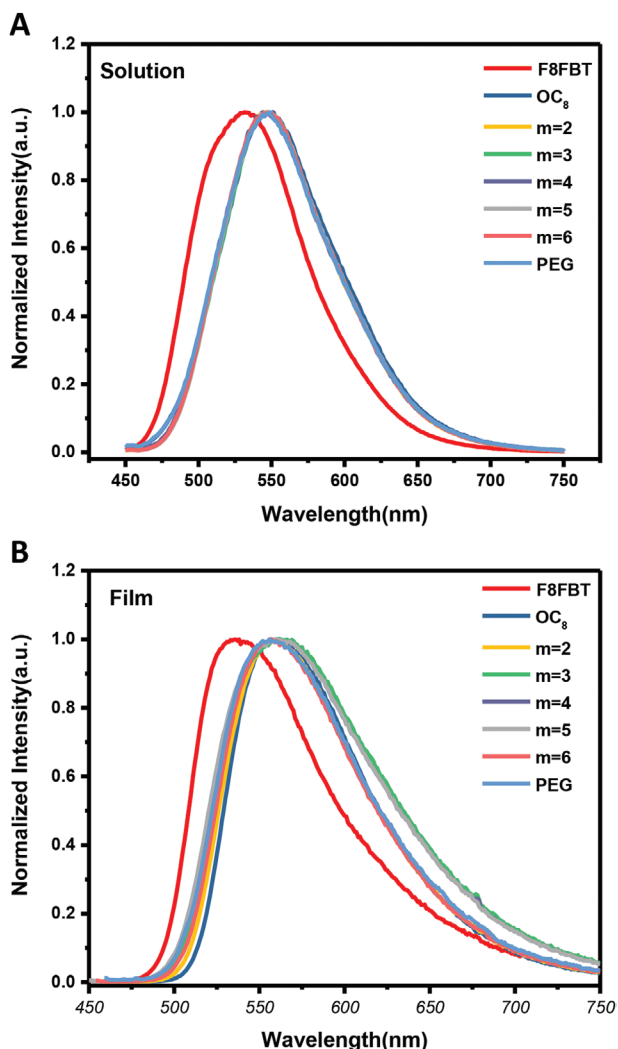
**Table 2.** Optical and electronic properties of polymers.

| Polymer | $\lambda_{abs, max}$ (sol)[nm] | $\lambda_{abs, max}$ (film) [nm] | $\lambda_{em, max}$ (sol) [nm] | $\lambda_{em, max}$ (film) [nm] | $E_{g(opt)}$ [eV] | HOMO [eV] (CV) |
|---|---|---|---|---|---|---|
| F8FBT | 319[a], 440[b] | 319[a], 452[b] | 532 | 538 | 2.45 | −6.07 |
| F8BT-OC$_8$ | 331[a], 445[b] | 334[a], 454[b] | 548 | 554 | 2.44 | −5.77 |
| F8BT-2 | 331[a], 442[b] | 335[a], 454[b] | 546 | 556 | 2.44 | −5.73 |
| F8BT-3 | 331[a], 442[b] | 335[a], 455[b] | 546 | 556 | 2.45 | −5.73 |
| F8BT-4 | 331[a], 442[b] | 336[a], 455[b] | 546 | 555 | 2.44 | −5.72 |
| F8BT-5 | 331[a], 442[b] | 335[a], 456[b] | 546 | 556 | 2.45 | −5.69 |
| F8BT-6 | 331[a], 442[b] | 336[a], 455[b] | 546 | 554 | 2.44 | −5.67 |
| F8BT-PEG | 331[a], 442[b] | 335[a], 454[b] | 546 | 550 | 2.46 | - |

[a] $\lambda_{max}$ of high energy band; [b] $\lambda_{max}$ of low energy band.

**Figure 2.** Emission spectra of polymers in chloroform solution a) and thin film b).

transition onset is seen at 154 °C with a peak at 138 °C. These transitions are similar to those observed in the unfluorinated F8BT polymer, in which the endotherms are ascribed to a transition to a liquid crystalline and isotropic phase.[47,55] After displacement of the fluoride from the conjugated backbone, the thermal properties of substituted polymers become very different, with no transitions observed between 30 °C and 300 °C, for F8BT-OC$_8$ and F8BT-m (m = 2–6), suggestive of amorphous materials. This is likely due to the additional steric bulk of the sidechains disrupting the packing of the conjugated backbones.

However, for F8BT-PEG we observed a strong endothermic transition on heating, which has an onset at 53 °C and peaks at 60 °C. The corresponding exotherm on cooling has an onset at 43 °C and peaks at 38 °C. These transitions are very close to the melting point and crystallization point for PEG$_{10K}$ (66 °C and 40 °C respectively).[56] Clearly, the PEG side chain plays a dominant role in the crystallinity and thermal behavior of F8BT-PEG.
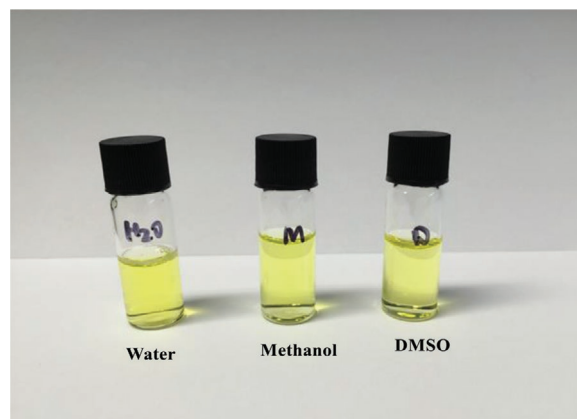


**Figure 3.** Photographs showing F8BT-PEG solubility in polar solvents (1 mg mL$^{-1}$).

## 2.4. Solubility and Wettability

The alkoxy-substituted F8BT-OC$_8$ and F8BT-m (m = 2, 3, 4, 5, 6) are all soluble in organic solvents, such as chloroform, THF, and chlorobenzene, but insoluble in polar solvents, such as methanol, acetonitrile, or water. However, the grafted F8BT-PEG is soluble in chloroform and THF, but also soluble in polar solvents, such as methanol, DMSO, or even pure water (**Figure 3**). The change of solubility is due to dominant effect of the grafted PEG$_{10K}$ chains.

In order to investigate the hydrophilicity of the substituted polymers more quantitatively, water was sequentially added to THF solutions of the polymers (2.5 mg mL$^{-1}$) at room temperature until a set transmittance was reached (65% of original transmittance) at 550 nm. This is a slight modification of a typical cloud point experiment, because although solutions of F8FBT, F8BT-OC$_8$, and F8BT-m (m = 2, 3, 4, 5, 6) became visibly cloudy as water was added, F8BT-6 did not, regardless of the amount of water added. Therefore the reduction in transmission at 550 nm due to scattering was taken to demonstrate the onset of precipitation. The data shown in **Table 3**, shows a systematic trend in which more water is required to cause precipitation as the length of the ethylene glycol sidechains increases, in agreement with an increase in polymer hydrophilicity. We note that F8BT-PEG is both water and THF soluble, and the transmittance of solution at 550 nm did not change when water added.

The change in hydrophility is further supported by contact angle measurements on polymer thin-films (**Figure 4**, Figure S5, Supporting Information, and Table 3). The contact angle of the parent F8FBT was 101.4°, similar to that of typical alkylated CPs.[57] Adding a hydrophobic alkyl sidechain resulted in little change (100.8° for F8BT-OC$_8$). The addition of the short ethylene glycol dimer did not significantly change the contact angle (F8BT-2), probably because the surface is still dominated by the octyl sidechains on the fluorene co-monomer. However, increasing the ethylene glycol sidechain length resulted in a systematic decrease in contact angle, from hydrophobic films to ambiphilic for F8BT-6 (85.6°). Furthermore, the contact angle for F8BT-PEG dropped dramatically to 31.0° (Figure 4). The contact angle of a pure PEG film is reported to be around

2000087 (5 of 8)

**ADVANCED
SCIENCE NEWS**

www.advancedsciencenews.com

**Macromolecular
Bioscience**

www.mbs-journal.de

**Table 3.** Hydrophilicity and contact angle.

| Polymer | Precipitation volume[a] v:v [%] | Contact angle[b] |
|---|---|---|
| F8FBT | 2.6 | 101.4±1.3° |
| F8BT-OC$_8$ | 4.6 | 100.8±1.1° |
| F8BT-2 | 12.9 | 99.7±1.3° |
| F8BT-3 | 15.3 | 92.9±1.6° |
| F8BT-4 | 28.6 | 92.0±1.6° |
| F8BT-5 | 41.9 | 90.9±1.4° |
| F8BT-6 | 45.3 | 85.6±1.0° |
| F8BT-PEG | - | 31.0±1.2° |

[a]Volume of water added to THF solution to produce 65% of original transmittance at 550 nm; [b]Average of five measurements

25°.[58] Clearly, the dramatic decrease of contact angle was due to the presence of the polymeric PEG sidechains.

Overall the solubility and contact angle data show that the hydrophilicity and wettability of the CPs can be modulated in a systematic way by nucleophilic aromatic substitution with ethylene glycol side chains. Importantly, such substitution does not affect the optoelectronic properties of the CP backbone.

## 3. Conclusion

A series of emissive CPs with increasingly hydrophilic side chains have been synthesized by nucleophilic aromatic substitution reactions on FBT monomer units within a CP backbone. Quantitative substitution of all fluoride was demonstrated with a series of monofunctionalized ethylene glycol oligomers, as well as with high molecular weight polyethylene glycol to afford a graft copolymer. The optical, electrical, and thermal properties of the resultant polymers were investigated. The length of the ethylene glycol sidechains was shown to have a direct impact on the surface wettability of the polymer, as well as its solubility in polar solvents. However, the energetics and band gap of the CPs remained essentially constant. This facile method therefore allows an easy way to modulate the wettability and solubility of

CP materials. More importantly, this convenient approach may open up a way to synthesize diverse CPs that can be used for bioelectronic applications.

## 4. Experimental Section

*CV Measurement*: CV was carried out with a standard three-electrode cell in a 0.1 M tetrabutylammonium hexafluorophosphate solution ((TBA)PF$_6$) in acetonitrile at room temperature with a scanning rate of 0.1 V s$^{-1}$. A Pt rod working electrode (1.6 mm diameter), a Pt wire counter electrode, and an Ag/AgCl reference electrode were used. The oxidation potentials were calibrated with a standard FOC redox system as the standard (assuming the energy level of FOC was 4.8 e V below vacuum) for estimating the HOMO energy level of polymers. Samples were prepared by drop-casting solution on the Pt rod surface.

*Solubility Measurement*: The transmittance of a THF solution (2.5 mg mL$^{-1}$) of the polymer was measured at 550 nm in a UV-1800 Shimadzu UV–vis spectrometer. Water was added portionwise until the transmittance dropped to 65% of the original value. The precipitation percentage was then calculated as volume H$_2$O/total volume (THF+H$_2$O).

*Contact Angle Measurement*: A Krüss DSA100E goniometer was used to carry out contact angle measurements using the static sessile drop method. All measurements took place at 25 °C at a humidity of 65%. Polymer solutions (5 mg mL$^{-1}$) were spin-coated onto quartz substrates at 2000 rpm. Prior to spin-coating, quartz substrates were washed sequentially by soap water, acetone, and isopropanol. Quartz substrates were then dried by flushing with nitrogen. For each measurement, a 5 µL drop of deionized water was suspended at the end of a needle and slowly brought into contact with the sample. Contact angles were measured 30 s after the withdrawal of the needle tip from the droplet to allow the drop time to equilibrate on the sample surface. Drop shapes were then fitted using the polynomial method. Each quoted contact angle was calculated from an average of five measurements made on the same sample.

*Synthesis—F8FBT*: A mixture of 9, 9-dioctyl-9*H*-fluorene-2, 7-diboronic acid bis (pinacol) ester (975.47 mg, 1.518 mmol), 4,7-dibromo-5-fluoro-2, 1,3-benzothiadiazole (473.42 mg, 1.518 mmol), tetrabutylammonium iodide (48 mg, 0.13 mmol), and Pd(PPh$_3$)$_4$ (35.1 mg, 0.0304 mmol) was added to a high pressure microwave vial. The vial was sealed with a septum and degassed with argon before toluene (10 mL) and K$_2$CO$_3$ (2 M, 4 mL) solution was added. The mixture was heated at 120 °C for 72 h. The reaction was cooled to room temperature and precipitated into methanol, stirred for 30 min, and filtered through a Soxhlet thimble. The precipitates were further purified by washing with methanol, acetone, and hexane under argon for 24 h, respectively. The remaining polymer
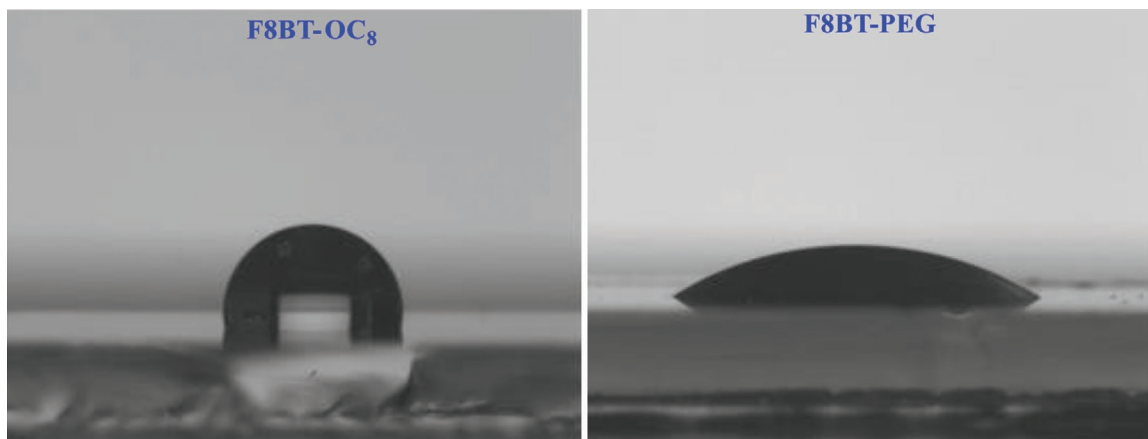


**Figure 4.** Water contact angle pictures of F8BT-OC$_8$ and F8BT-PEG.

in the thimble was then dissolved in hot chloroform and precipitated into methanol to give F8FBT as a fibrous yellow solid (591 mg, 72%). $M_n$: 38.5 kDa, $M_w$: 65.1 kDa, $M_w/M_n$ (Đ): 1.69. ^{1}H-NMR (400 MHz, CDCl$_3$, $\delta$): 8.15–7.79 (m, 7H, ArH), 2.16 (m, 4H, CH$_2$), 1.33–1.08 (m, 20H, CH$_2$), 0.99 (m, 4H, CH$_2$), 0.84 (m, 6H, CH$_3$). ^{19}F-NMR (400 MHz, CDCl$_3$) $\delta$ -114.5 ppm.

*General Procedure for Substituted Polymers*: A mixture of F8FBT (54 mg, 0.1 mmol) and KOH (112 mg, 2.0 mmol) was added to a high pressure microwave vial. The vial was sealed with a septum and degassed with argon before anhydrous chlorobenzene and DMSO (3:1, v:v, 8 ml total) and the desired alcohol (0.2 mmol) was added. The solution was heated at 120 °C for 48 h. During this time the reaction was monitored by NMR spectroscopy (^{1}H and ^{19}F) of quenched aliquots (quenched by precipitation into methanol, centrifugation and washing with acetone). After reaction, the solution was precipitated into methanol dropwise, stirred for 30 min, and filtered through a Soxhlet thimble. The precipitates were further purified by washing with acetone under argon for 24 h and the polymer was extracted with chloroform. The chloroform was removed under reduced pressure to afford the product.

*F8BT-OC$_8$*: $M_n$: 37.5 kDa, $M_w$: 74.2 kDa, $M_w/M_n$ (Đ): 1.98 ^{1}H-NMR (400 MHz, CDCl$_3$, $\delta$): 8.17–7.74 (m, 7H, ArH), 4.22 (m, 2H, CH$_2$), 2.17 (m, 4H, CH$_2$), 1.81 (m, 2H, CH$_2$), 1.44 (m, 2H, CH$_2$), 1.32 (m, 8H, CH, CH$_2$, CH$_3$), 1.19 (m, 20H, CH$_2$), 1.01 (m, 4H, CH$_2$), 0.92 (t, $J$ = 6.0 Hz, 3H, CH$_3$), 0.83 (t, $J$ = 6.0 Hz, 6H, CH$_3$). ^{19}F-NMR (400 MHz, CDCl$_3$) no fluorine signal.

*F8BT-2*: $M_n$: 45.4 kDa, $M_w$: 78.3 kDa, $M_w/M_n$ (Đ): 1.72 ^{1}H-NMR (400 MHz, CDCl$_3$, $\delta$): 8.23–7.72 (m, 7H, ArH), 4.39 (m, 2H, CH$_2$), 3.85 (m, 2H, CH$_2$), 3.68 (t, $J$ = 4.8 Hz, 2H, CH$_2$), 3.57 (t, $J$ = 4.4 Hz, 2H, CH$_2$), 3.39 (s, 3H, CH$_3$), 2.14 (m, 4H, CH$_2$), 1.19 (m, 20H, CH$_2$), 1.09–0.91 (m, 4H, CH$_2$), 0.83 (t, $J$ = 6.0 Hz, 6H, CH$_3$). ^{19}F-NMR (400 MHz, CDCl$_3$) no fluorine signal.

*F8BT-3*: $M_n$: 54.1 kDa, $M_w$: 89.3 kDa, $M_w/M_n$ (Đ): 1.65 ^{1}H-NMR (400 MHz, CDCl$_3$, $\delta$): 8.33–7.68 (m, 7H, ArH), 4.38 (m, 2H, CH$_2$), 3.86 (m, 2H, CH$_2$), 3.67 (m, 6H, CH$_2$), 3.54 (t, $J$ = 4.4 Hz, 2H, CH$_2$), 3.38 (s, 3H, CH$_3$), 2.18 (m, 4H, CH$_2$), 1.19 (m, 20H, CH$_2$), 0.99 (m, 4H, CH$_2$), 0.84 (t, $J$ = 6.2 Hz, 6H, CH$_3$). ^{19}F-NMR (400 MHz, CDCl$_3$) no fluorine signal.

*F8BT-4*: $M_n$: 55.2 kDa, $M_w$: 88.1 kDa, $M_w/M_n$ (Đ): 1.60 ^{1}H-NMR (400 MHz, CDCl$_3$, $\delta$): 8.26–7.73 (m, 7H, ArH), 4.38 (m, 2H, CH$_2$), 3.84 (m, 2H, CH$_2$), 3.76–3.59 (m, 10H, CH$_2$), 3.55 (t, $J$ = 4.2 Hz, 2H, CH$_2$), 3.38 (s, 3H, CH$_3$), 2.31–1.97 (m, 4H, CH$_2$), 1.19 (m, 20H, CH$_2$), 0.99 (m, 4H, CH$_2$), 0.83 (t, $J$ = 6.2 Hz, 6H, CH$_3$). ^{19}F-NMR (400 MHz, CDCl$_3$) no fluorine signal.

*F8BT-5*: $M_n$: 50.8 kDa, $M_w$: 83.9 kDa, $M_w/M_n$ (Đ): 1.65 ^{1}H-NMR (400 MHz, CDCl$_3$, $\delta$): 8.16–7.83 (m, 7H, ArH), 4.38 (m, 2H), 3.83 (m, 2H, CH$_2$), 3.74–3.60 (m, 14H, CH$_2$), 3.55 (m, 2H, CH$_2$), 3.38 (s, 3H, CH$_3$), 2.15 (m, 4H, CH$_2$), 1.19 (m, 20H, CH$_2$), 0.99 (m, 4H, CH$_2$), 0.82 (t, $J$ = 6.2 Hz, 6H, CH$_3$). ^{19}F-NMR (400 MHz, CDCl$_3$) no fluorine signal.

*F8BT-6*: $M_n$: 49.9 kDa, $M_w$: 85.4 kDa, $M_w/M_n$ (Đ): 1.71 ^{1}H-NMR (400 MHz, CDCl$_3$, $\delta$): 8.21–7.76 (m, 7H, ArH), 4.39 (m, 2H, CH$_2$), 3.85 (m, 2H, CH$_2$), 3.67 (m, 18H, CH$_2$), 3.56 (m, 2H, CH$_2$), 3.39 (s, 3H, CH$_3$), 2.14 (m, 4H, CH$_2$), 1.19 (m, 20H, CH$_2$), 0.99 (m, 4H, CH$_2$), 0.83 (t, $J$ = 6.2 Hz, 6H, CH$_3$). ^{19}F-NMR (400 MHz, CDCl$_3$) no fluorine signal.

*F8BT-PEG*: A mixture of F8FBT (10.8 mg, 0.02 mmol), poly(ethylene glycol) methyl ether (Mn 10 000 g mol$^{-1}$, Đ < 1.2, Aldrich 400 mg, 0.04 mmol) and KOH (22.4 mg, 0.4 mmol) was added to a high pressure microwave vial. The vial was sealed with a septum and degassed with argon before anhydrous chlorobenzene and DMSO (3:1, v:v, 10 mL total) were added. The solution was heated at 120 °C for 2 d. After reaction, the solvent was removed by distillation under reduced pressure, and the residue was dissolved in deionized water. Then the aqueous solution was injected into the dialysis cassettes by a syringe. The cassette was incubated in deionized water for 2 d with deionized water changed every 12 h. The resulting aqueous solution was dried to afford F8BT-PEG as a bright yellow powder (167 mg, 79% yield). ^{19}F-NMR (400 MHz, CDCl$_3$) shows no fluorine signal. ^{1}H-NMR (400 MHz, CDCl$_3$, $\delta$): 8.2–7.5 (m, 7H, ArH), 4–2.5 (br, s), 3.36 (s), 2.14 (m, 4H, CH$_2$), 1.4–1.0 (br m, 20H) 0.78 (br s, 6H).The peak intensity of the peaks arising from the F8BT

was very weak compared to the dominate PEG$_{10K}$ peaks (see Figure S6, Supporting Information) making accurate integrations difficult.

## Supporting Information

Supporting Information is available from the Wiley Online Library or from the author.

## Conflict of Interest

The authors declare no conflict of interest.

[1] D. Tuncel, H. V. Demir, *Nanoscale* **2010**, *2*, 484.

[2] L. H. Feng, C. L. Zhu, H. X. Yuan, L. B. Liu, F. T. Lv, S. Wang, *Chem. Soc. Rev.* **2013**, *42*, 6620.

[3] X. L. Feng, F. T. Lv, L. B. Liu, H. W. Tang, C. F. Xing, Q. O. Yang, S. Wang, *ACS Appl. Mater. Interfaces* **2010**, *2*, 2429.

[4] H. Bronstein, C. B. Nielsen, B. C. Schroeder, I. McCulloch, *Nat. Rev. Chem.*, **2020**, *4*, 66.

[5] M. Nikolka, G. Schweicher, J. Armitage, I. Nasrallah, C. Jellett, Z. J. Guo, M. Hurhangee, A. Sadhanala, I. McCulloch, C. B. Nielsen, H. Sirringhaus, *Adv. Mater.* **2018**, *30*, 1801874.

[6] M. Berggren, A. R. Dahlfors, *Adv. Mater.* **2007**, *19*, 3201.

[7] S. Inal, J. Rivnay, A. O. Suiu, G. G. Malliaras, I. McCulloch, *Acc. Chem. Res.* **2018**, *51*, 1368.

[8] J. B. Gonzalez, C. J. Kousseff, C. B. Nielsen, *J. Mater. Chem. C* **2019**, *7*, 1111.

[9] C. M. Yang, H. Frei, F. A. Rossi, H. M. Burt, *J. Tissue Eng. Regener. Med.* **2009**, *3*, 601.

[10] K. M. Persson, R. Karlsson, K. Svennersten, S. Loffler, E. W. H. Jager, A. R. Dahlfors, P. Konradsson, M. Berggren, *Adv. Mater.* **2011**, *23*, 4403.

[11] A. Giovannitti, D. T. Sbircea, S. Inal, C. B. Nielsen, E. Bandiello, D. A. Hanifi, M. Sessolo, G. G. Malliaras, I. McCulloch, J. Rivnay, *Proc. Natl. Acad. Sci. USA* **2016**, *113*, 12017.

[12] I. Uguz, C. M. Proctor, V. F. Curto, A. M. Pappa, M. J. Donahue, M. Ferro, R. M. Owens, D. Khodagholy, S. Inal, G. G. Malliaras, *Adv. Mater.* **2017**, *29*, 1701217.

[13] D. M. Kim, J. M. Moon, W. C. Lee, J. H. Yoon, C. S. Choi, Y. B. Shim, *Biosens. Bioelectron.* **2017**, *91*, 276.

[14] G. Z. Gao, D. Lange, K. Hilpert, J. Kindrachuk, Y. Q. Zou, J. T. J. Cheng, M. K. Narbat, K. Yu, R. Z. Wang, S. K. Straus, D. E. Brooks, B. H. Chew, R. E. W. Hancock, J. N. Kizhakkedathu, *Biomaterials* **2011**, *32*, 3899.

[15] J. Sekine, S. C. Luo, S. Wang, B. Zhu, H. R. Tseng, H. Yu, *Adv. Mater.* **2011**, *23*, 4788.

[16] J. Rivnay, R. M. Owens, G. G. Malliaras, *Chem. Mater.* **2014**, *26*, 679.

[17] R. A. Green, R. T. Hassarati, J. A. Goding, S. Baek, N. H. Lovell, P. J. Martens, L. A. Warren, *Macromol. Biosci.* **2012**, *12*, 494.

[18] B. Wenger, N. Tetreault, M. E. Welland, R. H. Friend, *Appl. Phys. Lett.* **2010**, *97*, 193303.

[19] L. Han, L. W. Yan, M. H. Wang, K. F. Wang, L. M. Fang, J. Zhou, J. Fang, F. Z. Ren, X. Lu, *Chem. Mater.* **2018**, *30*, 5561.

[20] Y. Q. Wang, B. Li, L. Z. Zeng, D. Cui, X. D. Xiang, W. S. Li, *Biosens. Bioelectron.* **2013**, *41*, 582.

[21] A. Savva, S. Wustoni, S. Inal, *J. Mater. Chem. C* **2018**, *6*, 12023.

[22] M. Moser, J. F. Ponder, A. Wadsworth, A. Giovannitti, I. McCulloch, *Adv. Funct. Mater.* **2019**, *29*, 1807033.

[23] E. Zeglio, O. Inganas, *Adv. Mater.* **2018**, *30*, 1800941.

[24] A. Giovannitti, I. P. Maria, D. Hanifi, M. J. Donahue, D. Bryant, K. J. Barth, B. E. Makdah, A. Savva, D. Moia, M. Zetek, P. R. F. Barnes, O. G. Reid, R. Inal, G. Rumbles, G. G. Malliaras, J. Nelson, J. Rivnay, I. McCulloch, *Chem. Mater.* **2018**, *30*, 2945.

[25] B. Meng, H. Y. Song, X. X. Chen, Z. Y. Xie, J. Liu, L. X. Wang, *Macromolecules* **2015**, *48*, 4357.

[26] B. Meng, J. Liu, L. Wang, *Polym. Chem.* **2020**, *11*, 1261.

[27] X. Chen, Z. Zhang, Z. Ding, J. Liu, L. Wang, *Angew. Chem., Int. Ed.* **2016**, *55*, 10376.

[28] S. Torabi, F. Jahani, I. Van Severen, C. Kanimozhi, S. Patil, R. W. A. Havenith, R. C. Chiechi, L. Lutsen, D. J. M. Vanderzande, T. J. Cleij, J. C. Hummelen, L. J. A. Koster, *Adv. Funct. Mater.* **2015**, *25*, 150.

[29] S. F. Yang, Z. T. Liu, Z. X. Cai, M. J. Dyson, N. Stingelin, W. Chen, H. J. Ju, G. X. Zhang, D. Q. Zhang, *Adv. Sci.* **2017**, *4*, 1700048.

[30] C. Kanimozhi, N. Y. Gross, E. K. Burnett, A. L. Briseno, T. D. Anthopoulos, U. Salzner, S. Patil, *Phys. Chem. Chem. Phys.* **2014**, *16*, 17253.

[31] D. C. Martin, *MRS Commun.* **2015**, *5*, 131.

[32] M. Golabi, A. P. F. Turner, E. W. H. Jager, *Sens. Actuators, B* **2016**, *222*, 839.

[33] K. M. Persson, S. Lonnqvist, K. Tybrandt, R. Gabrielsson, D. Nilsson, G. Kratz, M. Berggren, *Adv. Funct. Mater.* **2015**, *25*, 7056.

[34] K. Feron, R. Lim, C. Sherwood, A. Keynes, A. Brichta, P. C. Dastoor, *Int. J. Mol. Sci.* **2018**, *19*, 2382.

[35] C. J. Bettinger, R. Langer, J. T. Borenstein, *Angew. Chem., Int. Ed.* **2009**, *48*, 5406.

[36] S. M. Oliveira, W. L. Song, N. M. Alves, J. F. Mano, *Soft Matter* **2011**, *7*, 8932.

[37] Y. Arima, H. Iwata, *Biomaterials* **2007**, *28*, 3074.

[38] S. H. Oh, J. H. Lee, *Biomed. Mater.* **2013**, *8*, 014101.

[39] N. M. Alves, J. Shi, E. Oramas, J. L. Santos, H. Tomas, J. F. Mano, *J. Biomed. Mater. Res., Part A* **2009**, *91A*, 480.

[40] S. H. Kim, H. J. Ha, Y. K. Ko, S. J. Yoon, J. M. Rhee, M. S. Kim, H. B. Lee, G. Khang, *J. Biomater. Sci., Polym. Ed.* **2007**, *18*, 609.

[41] Q. Zhao, X. B. Zhou, T. Y. Cao, K. Y. Zhang, L. J. Yang, S. J. Liu, H. Liang, H. R. Yang, F. Y. Li, W. Huang, *Chem. Sci.* **2015**, *6*, 1825.

[42] Y. H. Chan, P. J. Wu, *Part. Part. Syst. Charact.* **2015**, *32*, 11.

[43] C. L. Zhu, L. B. Liu, Q. Yang, F. T. Lv, S. Wang, *Chem. Rev.* **2012**, *112*, 4687.

[44] C. A. Traina, R. C. Bakus, G. C. Bazan, *J. Am. Chem. Soc.* **2011**, *133*, 12600.

[45] A. Savva, R. Hallani, C. Cendra, J. Surgailis, T. C. Hidalgo, S. Wustoni, R. Sheelamanthula, X. X. Chen, M. Kirkus, A. Giovannitti, A. Salleo, I. McCulloch, S. Inal, *Adv. Funct. Mater.* **2020**, *30*, 1907657.

[46] A. Creamer, C. S. Wood, P. D. Howes, A. Casey, S. Y. Cong, A. V. Marsh, R. Godin, J. Panidi, T. D. Anthopoulos, C. H. Burgess, T. M. Wu, Z. P. Fei, I. Hamilton, M. A. McLachlan, M. M. Stevens, M. Heeney, *Nat. Commun.* **2018**, *9*, 3237.

[47] C. L. Donley, J. Zaumseil, J. W. Andreasen, M. M. Nielsen, H. Sirringhaus, R. H. Friend, J. S. Kim, *J. Am. Chem. Soc.* **2005**, *127*, 12890.

[48] W. K. Zhong, J. F. Liang, S. Z. Hu, X. F. Jiang, L. Ying, F. Huang, W. Yang, Y. Cao, *Macromolecules* **2016**, *49*, 5806.

[49] R. Q. Yang, R. Y. Tian, Q. Hou, W. Yang, Y. Cao, *Macromolecules* **2003**, *36*, 7453.

[50] A. Jerschow, N. Muller, *Macromolecules* **1998**, *31*, 6573.

[51] A. Creamer, A. Casey, A. V. Marsh, M. Shahid, M. Gao, M. Heeney, *Macromolecules* **2017**, *50*, 2736.

[52] Z. G. Zhang, Y. F. Li, *Sci. China: Chem.* **2015**, *58*, 192.

[53] W. B. Zhang, C. Wang, G. Liu, J. Wang, Y. Chen, R. W. Li, *Chem. Commun.* **2014**, *50*, 11496.

[54] C. M. Cardona, W. Li, A. E. Kaifer, D. Stockdale, G. C. Bazan, *Adv. Mater.* **2011**, *23*, 2367.

[55] M. J. Banach, R. H. Friend, H. Sirringhaus, *Macromolecules* **2003**, *36*, 2838.

[56] K. Pielichowski, K. Flejtuch, *Polym. Adv. Technol.* **2002**, *13*, 690.

[57] S. Yan, W. Li, H. Bi, M. Wang, D. Sun, Q. Wei, S. W. Wang, Z. Wang, M. Y. Zhang, *Chem. Commun.* **2019**, *55*, 3274.

[58] P. Kim, D. H. Kim, B. Kim, S. K. Choi, S. H. Lee, A. Khademhosseini, R. Langer, K. Y. Suh, *Nanotechnology* **2005**, *16*, 2420.

**2000087 (8 of 8)**